The bound polaron in a cylindrical quantum well wire with a finite confining potential

2000 J. Phys.: Condens. Matter 12 8623

(http://iopscience.iop.org/0953-8984/12/40/307)

J. Phys.: Condens. Matter **12** (2000) 8623–8640. Printed in the UK PII: S0953-8984(00)13915-3

The bound polaron in a cylindrical quantum well wire with a finite confining potential

Hong-Jing Xie†‡‖, Chuan-Yu Chen‡§ and Ben-Kun Ma†

† Department of Physics, Beijing Normal University, Beijing 100875, China
‡ Department of Physics, Guangzhou Normal University, Guangzhou 510400, China
§ CCAST (World Laboratory), PO Box 8730, Beijing 100080, China

E-mail: hjxie@guangztc.edu.cn (Hong-Jing Xie)

Received 16 May 2000, in final form 5 September 2000

Abstract. The phonon modes of a quantum well wire, formed by a cylindrical polar semiconductor 1 (well material) ($\rho < R_1$) embedded in another polar semiconductor 2 (barrier material) ($R_1 \leqslant \rho < R_2$), were studied by using the dielectric continuum model. The confined longitudinal optical phonon modes both in the wire (LO1) and in the barrier materials (LO2) and the interface optical (IO) phonon modes as well as the corresponding electron–phonon interaction Hamiltonians are derived. With a two-parameter variational trial wave function, the bound-polaron binding energy has been calculated numerically for different confining potential heights and wire radii. The result shows that the electron–phonon interaction can greatly modify the impurity binding energy. The IO modes are the main factor contributing to the modification. The influence of the LO1 modes increases as the wire radius increases and reaches the bulk limit at large wire radius, while the LO2 modes only show their influence at narrow wire radius.

1. Introduction

The progress in semiconductor nanotechnology has made it possible to fabricate various kinds of semiconductor heterostructure including many kinds of low-dimensional structure. The quantum well wire (QWW) system is one of the fields of great interest. Both experimental [1–3] and theoretical [4–6] studies on the electronic structure, transport properties, exciton and impurity levels and binding energies in QWW have been widely reported.

The properties of impurities have always been of great interest to researchers, since Bastard's pioneering work on the donor impurity in a semiconductor quantum well [6]. Many authors have extended their research to impurities in low-dimensional structures [7,8]. Brown and Spector [9] studied the hydrogen-like impurities in a QWW, considering both the infinite- and finite-confinement situations. Since it is impossible to obtain a formula solution to the Schrödinger equation for an impurity in a low-dimensional system, approximation methods have to be used; among these, the variational approach is the one most widely used. In our recent publication [10], we developed a two-parameter trial wave function especially tailored for the QWW structures. Calculation shows that it can obtain a better result than that given by Brown and Spector [9].

It is well known that the electron–optical phonon interaction is an important factor influencing the physical properties of polar crystals. The effect of such an influence

‖ Author to whom any correspondence should be addressed. Mailing address: Department of Physics, Guangzhou Normal University, Guangzhou 510400, China. Telephone: +86-20-86232187 (H); +86-20-86237563 (O).

0953-8984/00/408623+18$30.00

becomes stronger as the dimensionality of the system reduces [11]. Research on the polaron properties of a cylindrical quantum wire indicates the dependence of the polaron effect on the dimensionality of the structure [12]. Therefore, it is essential to consider the polaron effect when studying the impurity properties in low-dimensional structures [10, 13–15]. However, before we study the bound polaron in a QWW system, we have to work out the appropriate phonon modes and electron–phonon interaction Hamiltonians for the QWW system.

A number of authors have made great contributions in studying the phonon modes and the electron–phonon interaction in low-dimensional semiconductor structures [16–23]. The electron–phonon interaction in a dielectric confined system was first studied by Lucas *et al* [16] and Licari and Evrard [17] within the dielectric continuum model. Wendler [18] developed the framework of the theory of optical phonons and electron–phonon interaction for the spatially confined systems. Constantinou and Ridley [19] worked out the phonon modes in a GaAs/Al_xGa_{1-x}As quantum well wire. Wang and Lei [20] derived the confined phonon modes and surface phonon modes in a free-standing cylindrical quantum wire and studied their interaction with electron carriers. Li and Chen [21] derived the phonon modes and the electron–phonon interaction Hamiltonians for a free-standing cylindrical quantum dot. Considering both the electrostatic and mechanical boundary conditions, Klimin *et al* [22] and Fomin and Pokatilov [23] studied the phonon modes and deduced the Hamiltonian of electron–phonon interaction in multilayer polar structures.

It should be noted that the image potential induced by the charged particles may influence the properties of electrons in the quantum wire, especially when the quantum wire is narrow [24, 25]. It is found that, for a quantum wire with dielectric discontinuity, the hole–acceptor attraction potential has a non-Coulombic form [22, 26]. However, Wendler and Hartwig [27] studied the effect of the image potential on the binding energy of hydrogenic impurities in semiconductor quantum wells. They found that, when all image contributions (the mutual image potential between the hydrogenic impurity and the electron and the self-image potentials of the two particles) are taken into consideration, the image potential effects on the hydrogenic donor binding energy will be weak for donor positions in the centre of the quantum well. Therefore, for simplicity, in the present work, the influence of the image potential will not be considered.

In this paper, we will consider a QWW formed by a cylindrical polar semiconductor 1 (the well material, $\rho < R_1$) embedded in another polar semiconductor 2 (the barrier material, $R_1 \leqslant \rho < R_2$, with $R_2 \gg R_1$). Bennett *et al* [28] have worked out the confined and interface optical phonon modes in this QWW system. In fact, there exist two types of confined longitudinal optical phonon (LO) mode in this system, namely, one type of LO mode inside the wire (LO1) and another in the barrier material (LO2). Research on quantum well structures shows that the influence of the LO2 modes becomes obvious as the dimension of the well reduces [29, 30]. In this paper, we will work out all the phonon modes and the corresponding Fröhlich electron–phonon interaction Hamiltonian. We will use the dielectric continuum model because of its simplicity and efficiency for the GaAs/AlAs and GaAs/AlGaAs systems [19, 28].

In the following, firstly, in section 2, we will study the impurity binding energy of the QWW structure, using a two-parameter trial wave function. Then in section 3, we will derive the various phonon modes and electron–phonon interaction Hamiltonians in the QWW system. Afterwards, in section 4, the impurity binding energy, together with the influence of phonons, i.e., the bound-polaron binding energy will be studied. Numerical calculation and detailed discussion on bound-polaron properties are given in section 5. Finally, in section 6, we present a brief summary.

2. The impurity ground state

Consider a cylindrical quantum well wire consisting of GaAs ($\rho < R_1$) embedded in $Ga_{1-x}Al_xAs$ ($R_1 \leqslant \rho < R_2$). The impurity is located at $\rho_i = 0$ (taking the wire axis as the origin). Under the effective-mass approximation, the Hamiltonian of the system can be written as (neglecting the image effect)

$$H_e = -\frac{\hbar^2}{2m^*}\nabla^2 - \frac{e^2}{\epsilon r} + V(\rho) \tag{1}$$

with

$$V(\rho) = \begin{cases} U & \rho \geqslant R_1 \\ 0 & \rho < R_1. \end{cases}$$

Let us first consider the electron wave function in a cylindrical quantum well wire with no impurity present, i.e. find the solution to the following Schrödinger equation:

$$\frac{\hbar^2}{2m^*}\left[-\frac{1}{\rho}\frac{\partial}{\partial\rho}\left(\rho\frac{\partial}{\partial\rho}\right) - \frac{\partial^2}{\partial z^2}\right]\psi(\rho,z) + V(\rho)\psi(\rho,z) = E_0\psi(\rho,z). \tag{2}$$

The solution gives

$$\psi(\rho,z) = \begin{cases} N J_0(\alpha\rho)\exp[\mathrm{i}qz] & \rho < R_1 \\ N\dfrac{J_0(\alpha R_1)}{K_0(\beta R_1)}K_0(\beta\rho)\exp[\mathrm{i}qz] & \rho \geqslant R_1 \end{cases} \tag{3}$$

where

$$\alpha = \sqrt{2m^*E_0/\hbar^2}$$

$$\beta = \sqrt{2m^*(U - E_0)/\hbar^2}$$

and $J_0(x)$ and $K_0(x)$ are the zero-order Bessel function and modified Bessel function of the second kind, respectively. The energy level E_0 is obtained by solving the following equation:

$$\alpha J_1(\alpha R_1)K_0(\beta R_1) = \beta K_1(\beta R_1)J_0(\alpha R_1). \tag{4}$$

On the basis of the above result, considering the anisotropy of the quantum wire system, we propose a trial wave function with two variational parameters for equation (1):

$$\Phi(\rho,z) = N\exp\left[-\sqrt{\lambda^2\rho^2 + \mu^2 z^2}\right] \times \begin{cases} J_0(\alpha\rho) & \rho < R_1 \\ \dfrac{J_0(\alpha R_1)}{K_0(\beta R_1)}K_0(\beta\rho) & \rho \geqslant R_1 \end{cases} \tag{5}$$

where λ and μ are variational parameters characterizing the anisotropy in the ρ- and z-directions. N is the normalization constant defined by

$$\frac{4\pi\lambda}{\mu}N^2\left\{\int_0^{R_1} J_0^2(\alpha\rho)K_1(2\lambda\rho)\rho^2\,\mathrm{d}\rho + \frac{J_0^2(\alpha R_1)}{K_0^2(\beta R_1)}\int_{R_1}^{\infty} K_0^2(\beta\rho)K_1(2\lambda\rho)\rho^2\,\mathrm{d}\rho\right\} = 1 \tag{6}$$

where $K_1(x)$ is the second-kind modified Bessel function of first order.

The expectation value of H_e is given by

$$\langle\Phi(\rho,z)|H_e|\Phi(\rho,z)\rangle = T + U \tag{7}$$

with

$$
\begin{aligned}
T = &-\frac{\hbar^2\lambda^2}{2m^*} + \frac{\pi\lambda\alpha^2\hbar^2N^2}{m^*\mu}\int_0^{R_1} J_0^2(\alpha\rho)K_1(2\lambda\rho)\rho^2\,\mathrm{d}\rho \\
&- \frac{\pi\lambda\beta^2\hbar^2N^2}{m^*\mu}\frac{J_0^2(\alpha R_1)}{K_0^2(\beta R_1)}\int_{R_1}^{\infty} K_0^2(\beta\rho)K_1(2\lambda\rho)\rho^2\,\mathrm{d}\rho \\
&- \frac{4\pi\alpha\hbar^2\lambda^2N^2}{m^*\mu}\int_0^{R_1} J_0(\alpha\rho)J_1(\alpha\rho)K_0(2\lambda\rho)\rho\,\mathrm{d}\rho \\
&- \frac{4\pi\beta\hbar^2\lambda^2N^2}{m^*\mu}\frac{J_0^2(\alpha R_1)}{K_0^2(\beta R_1)}\int_{R_1}^{\infty} K_0(\beta\rho)K_1(\beta\rho)K_0(2\lambda\rho)\rho\,\mathrm{d}\rho \\
&+ \frac{2\pi\hbar^2\lambda N^2}{m^*\mu}\int_0^{R_1} J_0(\alpha\rho)\left[\alpha J_1(\alpha\rho) - \frac{1}{2}\alpha^2\rho J_2(\alpha\rho)\right]K_1(2\lambda\rho)\rho\,\mathrm{d}\rho \\
&+ \frac{2\pi\hbar^2\lambda N^2}{m^*\mu}\frac{J_0^2(\alpha R_1)}{K_0^2(\beta R_1)}\int_{R_1}^{\infty} K_0(\alpha\rho)\left[\beta K_1(\alpha\rho) - \frac{1}{2}\beta^2\rho K_2(\alpha\rho)\right] \\
&\times K_1(2\lambda\rho)\rho\,\mathrm{d}\rho \\
&+ \frac{4\pi\hbar^2\lambda^2N^2}{m^*\mu}\left[\int_0^{R_1} J_0^2(\alpha\rho)K_0(2\lambda\rho)\rho\,\mathrm{d}\rho\right. \\
&\left.+ \frac{J_0^2(\alpha R_1)}{K_0^2(\beta R_1)}\int_{R_1}^{\infty} K_0^2(\beta\rho)K_0(2\lambda\rho)\rho\,\mathrm{d}\rho\right] \\
&+ \frac{2\pi\hbar^2(\mu^2-\lambda^2)}{m^*}N^2\int_0^{R_1}\int_0^{\infty} J_0^2(\alpha\rho)\mu^2z^2\frac{\exp\left[-2\sqrt{\lambda^2\rho^2+\mu^2z^2}\right]}{\lambda^2\rho^2+\mu^2z^2}\rho\,\mathrm{d}\rho\,\mathrm{d}z \\
&+ \frac{2\pi\hbar^2(\mu^2-\lambda^2)}{m^*}N^2\frac{J_0^2(\alpha R_1)}{K_0^2(\beta R_1)} \\
&\times \int_{R_1}^{\infty}\int_0^{\infty} K_0^2(\alpha\rho)\mu^2z^2\frac{\exp\left[-2\sqrt{\lambda^2\rho^2+\mu^2z^2}\right]}{\lambda^2\rho^2+\mu^2z^2}\rho\,\mathrm{d}\rho\,\mathrm{d}z \qquad (8)
\end{aligned}
$$

and

$$
U = -\frac{4\pi N^2e^2}{\epsilon}\int\left[J_0\left(\frac{\chi_0^1\rho}{R}\right)\right]^2\frac{\exp\left[-2\sqrt{\lambda^2\rho^2+\mu^2z^2}\right]}{\sqrt{\rho^2+z^2}}\rho\,\mathrm{d}\rho\,\mathrm{d}z. \qquad (9)
$$

The ground-state energy of the impurity is obtained by minimizing the expectation value of the Hamiltonian H_e according to the variational parameters λ and μ:

$$
E = \min_{\mu,\lambda}\langle\Phi(\rho,z)|H_e|\Phi(\rho,z)\rangle. \qquad (10)
$$

The impurity binding energy is given by

$$
E_b = E_0 - E \qquad (11)
$$

where E_0 is the solution of equation (4).

3. The phonon modes and electron–phonon interaction Hamiltonians

In this section, we will use the dielectric continuum model to derive the various phonon modes and Fröhlich electron–phonon interaction Hamiltonians for the quantum well wire system. In the structure, material 1 lies within $\rho < R_1$ and material 2 fills up the space $R_1 \leqslant \rho < R_2$.

$R_2 \gg R_1$. In the following analysis, the periodic boundary condition along the z-direction is introduced: $-\frac{1}{2}L \leqslant z \leqslant \frac{1}{2}L$. Optical phonon modes in the structures are determined using classical electrostatics. We start with the electrostatic equations

$$\boldsymbol{\nabla} \cdot \boldsymbol{D} = 4\pi\rho_0(\boldsymbol{r}) \tag{12}$$

$$\boldsymbol{D} = \epsilon \boldsymbol{E} = \boldsymbol{E} + 4\pi \boldsymbol{P} \tag{13}$$

$$\boldsymbol{E} = -\boldsymbol{\nabla}\phi(\boldsymbol{r}) \tag{14}$$

where $\rho_0(\boldsymbol{r})$ is the charge density. For free oscillation (i.e. $\rho_0 = 0$), we have

$$\epsilon\, \nabla^2\phi(\boldsymbol{r}) = 0. \tag{15}$$

3.1. The confined LO modes

There are two solutions for equation (15). The first is $\epsilon = 0$ inside the wire. Since

$$\epsilon(\omega) = \epsilon_\infty + \frac{\epsilon_0 - \epsilon_\infty}{1 - \omega^2/\omega_{TO}^2} \tag{16}$$

we have that $\epsilon(\omega) = 0$ gives

$$\omega^2 = \omega_{TO}^2 \frac{\epsilon_0}{\epsilon_\infty} = \omega_{LO}^2 \tag{17}$$

in which we have made use of the Lyddane–Sachs–Teller (LST) relation; i.e. for the solution of $\epsilon(\omega) = 0$, we obtained a bulk LO phonon vibration mode.

3.1.1. Confined LO phonon modes inside the well (LO1). The potential for the confined LO mode inside the wire ($\rho \leqslant R_1$) can be chosen as

$$\phi_{ml}(\boldsymbol{r}) = \begin{cases} C_{ml} J_m(\chi_m^l \rho/R_1) \exp[\mathrm{i}m\varphi] \exp[\mathrm{i}q_z z] & \rho \leqslant R_1 \\ 0 & \rho > R_1 \end{cases} \tag{18}$$

where $J_m(x)$ is the Bessel function of the mth order, χ_m^l is the lth zero of $J_m(x)$.

The phonon mode described here is fundamentally identical to the one that we derived for the quantum wire in our recent paper [10]. So it is unnecessary to repeat the trivial algebraic calculation and we simply give the result here.

The phonon Hamiltonian of the LO1 mode is

$$H_{LO1} = \sum_{mlq_z} \hbar\omega_{LO1} \left[\hat{a}_{ml}^\dagger(q_z)\hat{a}_{ml}(q_z) + \frac{1}{2}\right] \tag{19}$$

where $\hat{a}_{ml}^\dagger(q_z)$ and $\hat{a}_{ml}(q_z)$ are the creation and annihilation operators for the LO1 phonon of the mlq_z-mode. They satisfy

$$\left[\hat{a}_{ml}(q_z), \hat{a}_{m'l'}^\dagger(q_z{}')\right] = \delta_{mm'}\delta_{ll'}\delta_{q_z q_z'} \tag{20}$$

$$\left[\hat{a}_{ml}(q_z), \hat{a}_{m'l'}(q_z{}')\right] = \left[\hat{a}_{ml}^\dagger(q_z), \hat{a}_{m'l'}^\dagger(q_z{}')\right] = 0 \tag{21}$$

and the Hamiltonian describing the interaction between the LO1 phonon and the electron is

$$H_{e-LO1} = -\sum_{mlq_z} \left[\Gamma_{ml}^{LO1}(q_z) J_m\left(\frac{\chi_m^l \rho}{R_1}\right) \mathrm{e}^{\mathrm{i}m\varphi} \mathrm{e}^{-\mathrm{i}q_z z} \hat{a}_{ml}^\dagger(q_z) + \mathrm{h.c.}\right] \tag{22}$$

where

$$|\Gamma_{ml}^{LO1}|^2 = \frac{4e^2\hbar\omega_{LO1}}{L J_{m+1}^2(\chi_m^l)(\chi_m^{l\,2} + R_1^2 q_z^2)} \left(\frac{1}{\epsilon_{\infty 1}} - \frac{1}{\epsilon_{01}}\right). \tag{23}$$

3.1.2. The LO mode in the barrier material (LO2). For the LO mode in the barrier material ($R_1 \leqslant \rho \leqslant R_2$), the potential for the LO2 mode can be chosen as

$$\phi_{ml}(\boldsymbol{r}) = \begin{cases} B_{ml} T_{ml}(a_{ml}\rho/R_1) \mathrm{e}^{\mathrm{i}m\varphi} \mathrm{e}^{\mathrm{i}q_z z} & R_1 \leqslant \rho \leqslant R_2 \\ 0 & \text{otherwise} \end{cases} \tag{24}$$

where

$$T_{ml}(a_{ml}\rho/R_1) = J_m(a_{ml}\rho/R_1) + b_{ml} Y_m(a_{ml}\rho/R_1). \tag{25}$$

$Y_m(x)$ is the second-kind Bessel function of order m. $T_{ml}(\rho)$ satisfies the boundary conditions at $\rho = R_1$ and $\rho = R_2$, i.e.

$$T_{ml}(a_{ml}\rho/R_1)\big|_{\rho=R_1} = T_{ml}(a_{ml}\rho/R_1)\big|_{\rho=R_2} = 0. \tag{26}$$

That is, a_{ml} and b_{ml} are the solutions to the equations

$$\begin{aligned} &J_m(a) + bY_m(a) = 0 \\ &J_m(aR_2/R_1) + bY_m(aR_2/R_1) = 0. \end{aligned} \tag{27}$$

$l = 0, 1, 2, \ldots$ denotes the number of zeros of $T_{ml}(a_{ml}\rho/R_1)$ within the range of $R_1 \leqslant \rho \leqslant R_2$.

We can prove that $T_{ml}(a_{ml}\rho/R_1)$ and $T_{mk}(a_{mk}\rho/R_1)$ are orthogonalized within the range of $R_1 \leqslant \rho \leqslant R_2$ (refer to appendix A).

The polarization vectors for the LO2 mode are

$$\begin{aligned} \boldsymbol{P}_{ml}^{LO_2} = \frac{1}{4\pi}\nabla\phi_{ml}(\boldsymbol{r}) = \frac{B_{ml}}{4\pi}\Bigg\{ &\frac{1}{2}[T_{m-1,l}(a_{ml}\rho/R_1) - T_{m+1,l}(a_{ml}\rho/R_1)]\frac{a_{ml}}{R_1}\boldsymbol{e}_\rho \\ &+ T_{ml}(a_{ml}\rho/R_1)\frac{\mathrm{i}m}{\rho}\boldsymbol{e}_\varphi + T_{ml}(a_{ml}\rho/R_1)\mathrm{i}q_z\Bigg\}\boldsymbol{e}_z \mathrm{e}^{\mathrm{i}m\varphi}\mathrm{e}^{\mathrm{i}q_z z}. \end{aligned} \tag{28}$$

Similarly to that for LO1 [10], The Hamiltonian of the free vibration is given by

$$H_{ph} = \frac{1}{2}\int [n\mu\dot{\boldsymbol{u}}\cdot\dot{\boldsymbol{u}} + n\mu\omega_0^2\boldsymbol{u}\cdot\boldsymbol{u} - ne\boldsymbol{u}\cdot\boldsymbol{E}_{loc}]\,\mathrm{d}^3 r. \tag{29}$$

Here μ is the reduced mass of the ion pair and $\boldsymbol{u} = \boldsymbol{u}_+ - \boldsymbol{u}_-$ is the relative displacement of the positive and negative ions, ω_0 is the frequency associated with the short-range force between ions, $\boldsymbol{E}_{loc}$ is the local field at the position of the ions, n is the number of ion pairs per unit volume and α is the electronic polarizability per ion pair.

Since

$$\boldsymbol{E}_{loc} = -\frac{8}{3}\pi\boldsymbol{P} \tag{30}$$

we have

$$\boldsymbol{u} = \frac{1 + \frac{8}{3}\pi n\alpha}{ne}\boldsymbol{P} \tag{31}$$

and then

$$H_{LO2} = \frac{1}{2}\int \left[n\mu\left(\frac{1 + \frac{8}{3}\pi n\alpha}{ne}\right)^2 \dot{\boldsymbol{P}}^*\cdot\dot{\boldsymbol{P}} + n\mu\omega_{LO2}^2\left(\frac{1 + \frac{8}{3}\pi n\alpha}{ne}\right)^2 \boldsymbol{P}^*\cdot\boldsymbol{P}\right] \mathrm{d}^3 r \tag{32}$$

since

$$\int \boldsymbol{P}_{ml}^{LO2*}(q_z)\cdot\boldsymbol{P}_{m'l'}^{LO2}(q_z')\,\mathrm{d}\boldsymbol{r} = \frac{LB_{ml}^2}{32\pi}\{a_{ml}^2[\gamma^2T_{m-1,l}^2(a_{ml}\gamma)+\gamma^2T_{m+1,l}^2(a_{ml}\gamma)-T_{m-1,l}^2(a_{ml})-T_{m+1,l}^2(a_{ml})] - 2q_z^2[R_2^2T_{m-1,l}(a_{ml}\gamma)T_{m+1,l}(a_{ml}\gamma)-R_1^2T_{m-1,l}(a_{ml})T_{m+1,l}(a_{ml})]\} \times \delta_{mm'}\delta_{ll'}\delta_{q_zq_z'} \tag{33}$$

where $\gamma = R_2/R_1$.

If we choose B_{ml} to be

$$B_{ml}^2 = \frac{32\pi}{n\mu L}\left(\frac{ne}{1+\frac{8}{3}\pi n\alpha}\right)^2\{a_{ml}^2[\gamma^2T_{m-1,l}^2(a_{ml}\gamma)+\gamma^2T_{m+1,l}^2(a_{ml}\gamma) - T_{m-1,l}^2(a_{ml})-T_{m+1,l}^2(a_{ml})]-2q_z^2[R_2^2T_{m-1,l}(a_{ml}\gamma)T_{m+1,l}(a_{ml}\gamma) - R_1^2T_{m-1,l}(a_{ml})T_{m+1,l}(a_{ml})]\}^{-1} \tag{34}$$

then $\boldsymbol{P}_{ml}^{LO2}$ may form an orthonormal and complete set, which can be used to express $\boldsymbol{P}$ as

$$\boldsymbol{P} = \sum_{mlq_z}\left(\frac{\hbar}{\omega_{LO2}}\right)^{1/2}\left[\hat{b}_{ml}(q_z)+\hat{b}_{ml}^{\dagger}(q_z)\right]\boldsymbol{P}_{ml}^{LO2}(\boldsymbol{r}) \tag{35}$$

$$\dot{\boldsymbol{P}} = -\mathrm{i}\sum_{mlq_z}(\hbar\omega_{LO2})^{1/2}\left[\hat{b}_{ml}(q_z)-\hat{b}_{ml}^{\dagger}(q_z)\right]\boldsymbol{P}_{ml}^{LO2}(\boldsymbol{r}). \tag{36}$$

$\boldsymbol{P}$ and $\dot{\boldsymbol{P}}$ are now quantum field operators; $\hat{b}_{ml}^{\dagger}(q_z)$ and $\hat{b}_{ml}(q_z)$ are the creation and annihilation operators for the LO2 phonon of the mlq_z-mode. They satisfy

$$\left[\hat{b}_{ml}(q_z),\hat{b}_{m'l'}^{\dagger}(q_z{}')\right] = \delta_{mm'}\delta_{ll'}\delta_{q_zq_z'} \tag{37}$$

$$\left[\hat{b}_{ml}(q_z),\hat{b}_{m'l'}(q_z{}')\right] = \left[\hat{b}_{ml}^{\dagger}(q_z),\hat{b}_{m'l'}^{\dagger}(q_z{}')\right] = 0. \tag{38}$$

Then the Hamiltonian operator for confined LO phonons will be

$$H_{LO2} = \sum_{mlq_z}\hbar\omega_{LO2}\left[\hat{b}_{ml}^{\dagger}(q_z)\hat{b}_{ml}(q_z)+\frac{1}{2}\right]. \tag{39}$$

The Hamiltonian describing the interaction between the electron and the phonon field is

$$H_{e-ph} = -e\phi(\boldsymbol{r}). \tag{40}$$

$\phi(\boldsymbol{r})$ can be expanded in terms of the normal modes, so

$$H_{e-LO2} = -\sum_{mlq_z}\left[\Gamma_{ml}^{LO2}(q_z)T_{ml}(a_{ml}\rho/R_1)\mathrm{e}^{\mathrm{i}m\varphi}\mathrm{e}^{-\mathrm{i}q_zz}\hat{b}_{ml}^{\dagger}(q_z)+\mathrm{h.c.}\right] \tag{41}$$

where

$$\Gamma_{ml}^{LO2}(q_z) = \sqrt{\frac{8e^2\hbar\omega_{LO2}}{L}}\left(\frac{1}{\epsilon_{\infty 2}}-\frac{1}{\epsilon_{02}}\right)^{1/2}\{a_{ml}^2[\gamma^2T_{m-1,l}^2(a_{ml}\gamma)+\gamma^2T_{m+1,l}^2(a_{ml}\gamma) - T_{m-1,l}^2(a_{ml})-T_{m+1,l}^2(a_{ml})]-2q_z^2[R_2^2T_{m-1,l}(a_{ml}\gamma)T_{m+1,l}(a_{ml}\gamma) - R_1^2T_{m-1,l}(a_{ml})T_{m+1,l}(a_{ml})]\}^{-1/2}. \tag{42}$$

3.2. The interface phonon modes

The other solution for equation (15) is

$$\nabla^2\phi(\boldsymbol{r}) = 0. \tag{43}$$

This will give the interface modes; the solution for equation (43) is

$$\phi_m(\boldsymbol{r}) = C_m \mathrm{e}^{\mathrm{i}m\varphi}\mathrm{e}^{\mathrm{i}q_z z}\begin{cases} K_m(q_z R_1)I_m(q_z\rho) & \rho \leqslant R_1 \\ I_m(q_z R_1)K_m(q_z\rho) & \rho > R_1 \end{cases} \tag{44}$$

where $K_m(x)$ and $I_m(x)$ are the modified Bessel functions of the first and second kind, respectively.

It should be noticed that

$$\epsilon_1(\omega) = \epsilon_{\infty 1}\frac{\omega^2 - \omega_{LO1}^2}{\omega^2 - \omega_{TO1}^2} \tag{45}$$

$$\epsilon_2(\omega) = \epsilon_{\infty 2}\frac{\omega^2 - \omega_{LO2}^2}{\omega^2 - \omega_{TO2}^2}. \tag{46}$$

The boundary condition at $\rho = R_1$ is

$$\epsilon_1(\omega)\frac{\partial\phi_1}{\partial\rho} = \epsilon_2(\omega)\frac{\partial\phi_2}{\partial\rho}.$$

This gives the dispersion relation

$$\epsilon_{\infty 1}\frac{\omega^2 - \omega_{LO1}^2}{\omega^2 - \omega_{TO1}^2}K_m(q_z R_1)\left[I_{m-1}(q_z R_1) + I_{m+1}(q_z R_1)\right] + \epsilon_{\infty 2}\frac{\omega^2 - \omega_{LO2}^2}{\omega^2 - \omega_{TO2}^2}I_m(q_z R_1)\left[K_{m-1}(q_z R_1) + K_{m+1}(q_z R_1)\right] = 0 \tag{47}$$

where

$$\omega_{\pm} = \left(\frac{-B \pm \sqrt{B^2 - 4AC}}{2A}\right)^{1/2} \tag{48}$$

with

$$A = \epsilon_{\infty 1}K_m(q_z R_1)\left[I_{m-1}(q_z R_1) + I_{m+1}(q_z R_1)\right] + \epsilon_{\infty 2}I_m(q_z R_1)\left[K_{m-1}(q_z R_1) + K_{m+1}(q_z R_1)\right]$$

$$B = \begin{cases} \dfrac{q_z R_1}{2m}\{[(\epsilon_{01} + \epsilon_{\infty 2})\omega_{TO1}^2 + (\epsilon_{02} + \epsilon_{\infty 1})\omega_{TO2}^2] \\ \quad \times [K_{m-1}(q_z R_1)I_{m-1}(q_z R_1) - K_{m+1}(q_z R_1)I_{m+1}(q_z R_1)] \\ \quad + [(\epsilon_{01} - \epsilon_{\infty 2})\omega_{TO1}^2 - (\epsilon_{02} - \epsilon_{\infty 1})\omega_{TO2}^2] \\ \quad \times [K_{m-1}(q_z R_1)I_{m+1}(q_z R_1) - K_{m+1}(q_z R_1)I_{m-1}(q_z R_1)]\} & \text{if } m \neq 0 \\ \{-2K_0(q_z R_1)I_1(q_z R_1)(\epsilon_{01}\omega_{TO1}^2 + \epsilon_{\infty 1}\omega_{TO2}^2) \\ \quad - 2I_0(q_z R_1)K_1(q_z R_1)(\epsilon_{02}\omega_{TO2}^2 + \epsilon_{\infty 2}\omega_{TO1}^2)\} & \text{if } m = 0 \end{cases}$$

$$C = \omega_{TO1}^2\omega_{TO2}^2\{\epsilon_{01}K_m(q_z R_1)[I_{m-1}(q_z R_1) + I_{m+1}(q_z R_1)] + \epsilon_{02}I_m(q_z R_1)[K_{m-1}(q_z R_1) + K_{m+1}(q_z R_1)]\}.$$

When ω is worked out, $\epsilon_1(\omega)$ and $\epsilon_2(\omega)$ can be obtained via equations (45) and (46) respectively.

The polarization fields for the IO phonon modes are

$$\boldsymbol{P}_m^{IO} = C_m \begin{cases} \dfrac{1-\epsilon_1}{4\pi}\,\boldsymbol{\nabla}\left[K_m(q_zR_1)I_m(q_z\rho)\mathrm{e}^{\mathrm{i}m\varphi}\mathrm{e}^{\mathrm{i}q_zz}\right] & \rho \leqslant R_1 \\ \dfrac{1-\epsilon_2}{4\pi}\,\boldsymbol{\nabla}\left[I_m(q_zR_1)K_m(q_z\rho)\mathrm{e}^{\mathrm{i}m\varphi}\mathrm{e}^{\mathrm{i}q_zz}\right] & \rho > R_1 \end{cases}$$

$$= C_m\mathrm{e}^{\mathrm{i}m\varphi}\mathrm{e}^{\mathrm{i}q_zz}\begin{cases} \dfrac{1-\epsilon_1}{4\pi}K_m(q_zR_1) \\ \qquad\times\left\{\dfrac{1}{2}q_z[I_{m-1}(q_z\rho)+I_{m+1}(q_z\rho)]\boldsymbol{e}_\rho\right. \\ \qquad\left.+\dfrac{\mathrm{i}m}{\rho}I_m(q_z\rho)\boldsymbol{e}_\varphi+\mathrm{i}q_zI_m(q_z\rho)\boldsymbol{e}_z\right\} & \rho \leqslant R_1 \\ \dfrac{1-\epsilon_2}{4\pi}I_m(q_zR_1) \\ \qquad\times\left\{\dfrac{1}{2}q_z[K_{m-1}(q_z\rho)+K_{m+1}(q_z\rho)]\boldsymbol{e}_\rho\right. \\ \qquad\left.+\dfrac{\mathrm{i}m}{\rho}K_m(q_z\rho)\boldsymbol{e}_\varphi+\mathrm{i}q_zK_m(q_z\rho)\boldsymbol{e}_z\right\} & \rho > R_1. \end{cases} \tag{49}$$

Similarly to in our previous paper [10], we obtain the Hamiltonian for the IO phonon:

$$H_{IO} = \frac{1}{2}\int \mathrm{d}^3r\left[n\mu\left(\frac{1}{ne[1+(\alpha\mu/e^2)(\omega_0^2-\omega^2)]}\right)^2\dot{\boldsymbol{P}}^*\cdot\dot{\boldsymbol{P}}\right.$$
$$\left.+\,n\mu\omega^2\left(\frac{1}{ne[1+(\alpha\mu/e^2)(\omega_0^2-\omega^2)]}\right)^2\boldsymbol{P}^*\cdot\boldsymbol{P}\right] \tag{50}$$

since

$$\int \boldsymbol{P}_{m'}^{IO*}(q_z')\cdot\boldsymbol{P}_m^{IO}(q_z)\,\mathrm{d}^3r = \frac{L}{16\pi}C_m^2\{(1-\epsilon_1)^2K_m^2(q_zR_1)I_m(q_zR_1)q_zR_1$$
$$\times[I_{m-1}(q_zR_1)-I_{m+1}(q_zR_1)]+2(1-\epsilon_2)^2I_m^2(q_zR_1)K_m(q_zR_1)$$
$$\times[K_{m+1}(q_zR_1)q_zR_1-mK_m(q_zR_1)]\}\delta_{mm'}\delta_{q_zq_z'}. \tag{51}$$

If we choose C_m as

$$C_m^{-2} = \frac{L}{4\omega^2}\left\{\left(\frac{1}{\epsilon_1-\epsilon_{01}}-\frac{1}{\epsilon_1-\epsilon_{\infty1}}\right)^{-1}\right.$$
$$\times K_m^2(q_zR_1)I_m(q_zR_1)q_zR_1[I_{m-1}(q_zR_1)-I_{m+1}(q_zR_1)]$$
$$+\,2I_m^2(q_zR_1)K_m(q_zR_1)[K_{m+1}(q_zR_1)q_zR_1-mK_m(q_zR_1)]$$
$$\left.\times\left(\frac{1}{\epsilon_2-\epsilon_{02}}-\frac{1}{\epsilon_2-\epsilon_{\infty2}}\right)^{-1}\right\} \tag{52}$$

then the $\boldsymbol{P}_m^{IO}$ may form an orthonormal and complete set. We may express $\boldsymbol{P}$ as

$$\boldsymbol{P} = \sum_{mq_z}\left(\frac{\hbar}{\omega}\right)^{1/2}[\hat{c}_m(q_z)+\hat{c}_m^\dagger(q_z)]\boldsymbol{P}_m^{IO2} \tag{53}$$

$$\dot{\boldsymbol{P}} = -\mathrm{i}\sum_{mq_z}(\hbar\omega)^{1/2}[\hat{c}_m(q_z)-\hat{c}_m^\dagger(q_z)]\boldsymbol{P}_m^{IO2} \tag{54}$$

where $\hat{c}_m^\dagger(q_z)$ and $\hat{c}_m(q_z)$ are the creation and annihilation operators for an IO phonon with frequency ω. They satisfy

$$\left[\hat{c}_m(q_z),\hat{c}_{m'}^\dagger(q_z')\right] = \delta_{mm'}\delta_{q_zq_z'} \tag{55}$$

$$\left[\hat{c}_m(q_z), \hat{c}_{m'}(q_z')\right] = \left[\hat{c}_m^\dagger(q_z), \hat{c}_{m'}^\dagger(q_z')\right] = 0. \tag{56}$$

The Hamiltonian operator for the IO phonons is

$$H_{IO} = \sum_{mq_z} \hbar\omega \left[\hat{c}_m^\dagger(q_z)\hat{c}_m(q_z) + \frac{1}{2}\right] \tag{57}$$

and the Hamiltonian describing the interaction between the electron and the IO phonon is

$$H_{e-IO} = -\sum_{mq_z} \left[\Gamma_m^{IO}(q_z)\mathrm{e}^{\mathrm{i}m\varphi}\mathrm{e}^{-\mathrm{i}q_z z}\hat{c}_m^\dagger(q_z) + \text{h.c.}\right] \times \begin{cases} K_m(q_z R_1) I_m(q_z \rho) & \rho \leqslant R_1 \\ I_m(q_z R_1) K_m(q_z \rho) & \rho > R_1 \end{cases} \tag{58}$$

where

$$\begin{aligned} |\Gamma_m^{IO}(q_z)|^2 &= C_m^2 \frac{e^2\hbar}{\omega} \\ &= \frac{4e^2\hbar\omega}{L}\left\{\left(\frac{1}{\epsilon_1 - \epsilon_{01}} - \frac{1}{\epsilon_1 - \epsilon_{\infty 1}}\right)^{-1}\right. \\ &\quad \times K_m^2(q_z R_1) I_m(q_z R_1) q_z R_1 [I_{m-1}(q_z R_1) - I_{m+1}(q_z R_1)] \\ &\quad + 2 I_m^2(q_z R_1) K_m(q_z R_1)[K_{m+1}(q_z R_1) q_z R_1 - m K_m(q_z R_1)] \\ &\quad \left.\times \left(\frac{1}{\epsilon_2 - \epsilon_{02}} - \frac{1}{\epsilon_2 - \epsilon_{\infty 2}}\right)^{-1}\right\}^{-1}. \end{aligned} \tag{59}$$

4. The bound-polaron binding energy

Now we consider the polaron effect on the impurity state (which is known as the bound-polaron state). The Hamiltonian of the system can be written as

$$H = H_e + H_{ph} + H_{e-ph} \tag{60}$$

where H_e, which is the impurity Hamiltonian, is given in equation (1). The second term is the phonon Hamiltonian:

$$\begin{aligned} H_{ph} &= H_{LO1} + H_{LO2} + H_{IO} \\ &= \sum_{mlq_z} \hbar\omega_{LO1}\left[a_{ml}^\dagger(q_z) a_{ml}(q_z) + \frac{1}{2}\right] + \sum_{mlq_z} \hbar\omega_{LO2}\left[b_{ml}^\dagger(q_z) b_{ml}(q_z) + \frac{1}{2}\right] \\ &\quad + \sum_{mq_z} \hbar\omega\left[c_m^\dagger(q_z) c_m(q_z) + \frac{1}{2}\right] \end{aligned} \tag{61}$$

and the third term is the electron–phonon interaction Hamiltonian given by

$$H_{e-ph} = H_{e-LO1} + H_{e-LO2} + H_{e-IO} \tag{62}$$

in which H_{e-LO1}, H_{e-LO2} and H_{e-IO} are given by equations (22), (41) and (58) respectively. We will use the variational method in our calculation. The trial wave function is chosen to be

$$|\Psi\rangle = \Phi(\rho, z) S |0\rangle. \tag{63}$$

$\Phi(\rho, z)$ is given in equation (5), $|0\rangle$ is the phonon vacuum state, while S is the second LLP transform defined by

$$\begin{aligned} S = \exp\Bigg[&\sum_{mlq_z} (f_{ml}^{LO1}(q_z) a_{ml}^\dagger(q_z) - f_{ml}^{LO1*}(q_z) a_{ml}(q_z)) \\ &+ \sum_{mlq_z} (f_{ml}^{LO2}(q_z) b_{ml}^\dagger(q_z) - f_{ml}^{LO2*}(q_z) b_{ml}(q_z)) \\ &+ \sum_{mq_z} (f_m^{IO}(q_z) c_m^\dagger(q_z) - f_m^{IO*}(q_z) c_m(q_z))\Bigg]. \end{aligned} \tag{64}$$

The first LLP transform is not applied here for the following reasons: (i) because of the existence of the Coulomb impurity, the total momentum of the system is no longer conserved; (ii) the strong confinement of the electron and phonons makes the coupling between them stronger [10]. The unitary operator S transforms the phonon operator as follows and hence H will be diagonalized:

$$S^{\dagger}a_{ml}^{\dagger}(q_z)S = a_{ml}^{\dagger}(q_z) + f_{ml}^{LO1*}(q_z)$$
$$S^{\dagger}a_{ml}(q_z)S = a_{ml}(q_z) + f_{ml}^{LO1}(q_z)$$

$$S^{\dagger}b_{ml}^{\dagger}(q_z)S = b_{ml}^{\dagger}(q_z) + f_{ml}^{LO2*}(q_z)$$
$$S^{\dagger}b_{ml}(q_z)S = b_{ml}(q_z) + f_{ml}^{LO2}(q_z)$$

$$S^{\dagger}c_{m}^{\dagger}(q_z)S = c_{m}^{\dagger}(q_z) + f_{m}^{IO*}(q_z)$$
$$S^{\dagger}c_{m}(q_z)S = c_{m}(q_z) + f_{m}^{IO}(q_z).$$

The expectation value of H is

$$\begin{aligned}\langle\Psi|H|\Psi\rangle = T + U &+ \sum_{mlq_z}|f_{ml}^{LO1}(q_z)|^2 + \sum_{mlq_z}|f_{ml}^{LO2}(q_z)|^2 + \sum_{mq_z}|f_{m}^{IO}(q_z)|^2 \\ &+ \sum_{mlq_z}[\Gamma_{ml}^{LO1}(q_z)\langle\Phi(\rho,z)|J_m(\chi_m^l\rho/R_1)\mathrm{e}^{\mathrm{i}m\varphi}\mathrm{e}^{-\mathrm{i}q_z z}|\Phi(\rho,z)\rangle + \text{h.c.}] \\ &+ \sum_{mlq_z}[\Gamma_{ml}^{LO2}(q_z)\langle\Phi(\rho,z)|T_{ml}(a_{ml}\rho/R_1)\mathrm{e}^{\mathrm{i}m\varphi}\mathrm{e}^{-\mathrm{i}q_z z}|\Phi(\rho,z)\rangle + \text{h.c.}] \\ &+ \sum_{mq_z}[\Gamma_{m}^{IO}(q_z)\langle\Phi(\rho,z)|g(q_z,\rho)\mathrm{e}^{\mathrm{i}m\varphi}\mathrm{e}^{-\mathrm{i}q_z z}|\Phi(\rho,z)\rangle + \text{h.c.}] \qquad (65)\end{aligned}$$

where

$$g(q_z,\rho) = \begin{cases} K_m(q_z R)I_m(q_z\rho) & \rho \leqslant R_1 \\ I_m(q_z R)K_m(q_z\rho) & \rho > R_1 \end{cases} \qquad (66)$$

Minimizing $\langle\Psi|H|\Psi\rangle$ with respect to $f_{ml}^{LO1*}(q_z)$, $f_{ml}^{LO2*}(q_z)$ and $f_{m}^{IO*}(q_z)$ successively, one obtains

$$f_{ml}^{LO1}(q_z) = -\Gamma_{ml}^{LO1}(q_z)\langle\Phi(\boldsymbol{r})|J_m(\chi_m^l\rho/R_1)\mathrm{e}^{\mathrm{i}m\varphi}\mathrm{e}^{-\mathrm{i}q_z z}|\Phi(\boldsymbol{r})\rangle \qquad (67)$$

$$f_{ml}^{LO2}(q_z) = -\Gamma_{ml}^{LO2}(q_z)\langle\Phi(\boldsymbol{r})|T_{ml}(a_{ml}\rho/R_1)\mathrm{e}^{\mathrm{i}m\varphi}\mathrm{e}^{-\mathrm{i}q_z z}|\Phi(\boldsymbol{r})\rangle \qquad (68)$$

$$f_{m}^{IO}(q_z) = -\Gamma_{m}^{IO}(q_z)\langle\Phi(\boldsymbol{r})|g(q_z,\rho)\mathrm{e}^{\mathrm{i}m\varphi}\mathrm{e}^{-\mathrm{i}q_z z}|\Phi(\boldsymbol{r})\rangle. \qquad (69)$$

Inserting equations (67), (68) and (69) into equation (65), we get

$$\langle\Psi|H|\Psi\rangle = T + U - \Delta E_{LO1} - \Delta E_{LO2} - \Delta E_{IO} \qquad (70)$$

with

$$\Delta E_{LO1} = \sum_{mlq_z}\frac{1}{\hbar\omega_{LO1}}|\Gamma_{ml}^{LO1}(q_z)|^2\left|\langle\Phi(\boldsymbol{r})|J_m(\chi_m^l\rho/R_1)\mathrm{e}^{\mathrm{i}m\varphi}\mathrm{e}^{-\mathrm{i}q_z z}|\Phi(\boldsymbol{r})\rangle\right|^2 \qquad (71)$$

$$\Delta E_{LO2} = \sum_{mlq_z}\frac{1}{\hbar\omega_{LO2}}|\Gamma_{ml}^{LO2}(q_z)|^2\left|\langle\Phi(\boldsymbol{r})|T_{ml}(a_{ml}\rho/R_1)\mathrm{e}^{\mathrm{i}m\varphi}\mathrm{e}^{-\mathrm{i}q_z z}|\Phi(\boldsymbol{r})\rangle\right|^2 \qquad (72)$$

and

$$\Delta E_{IO} = \sum_{mq_z}\frac{1}{\hbar\omega}|\Gamma_{m}^{IO}(q_z)|^2\left|\langle\Phi(\boldsymbol{r})|g(q_z,\rho)\mathrm{e}^{\mathrm{i}m\varphi}\mathrm{e}^{-\mathrm{i}q_z z}|\Phi(\boldsymbol{r})\rangle\right|^2. \qquad (73)$$

T and U are defined in equations (8) and (9) respectively. The ground-state energy of the system is calculated using equation (70):

$$E = \min_{\lambda,\mu} \langle \Psi | H | \Psi \rangle. \tag{74}$$

The impurity binding energy with the phonon contribution is calculated using equation (11) with E obtained above.

5. Results and discussion

Numerical calculations were carried out on the GaAs–$Ga_{1-x}Al_xAs$ quantum well quantum wire. The material parameters are listed in table 1.

Table 1. The material parameters.

	Material parameters [11, 31]		
	GaAs ($\nu = 1$)	$Ga_{1-x}Al_xAs$ ($\nu = 2$)	AlAs
m_ν (units of m_0)	0.067	$0.067 + 0.083x$	0.15
$\hbar\omega_{LO\nu}$ (meV)	36.25	$36.25 + 3.83x + 17.12x^2 - 5.11x^3$	50.09
$\hbar\omega_{TO\nu}$ (meV)	33.29	$33.29 + 10.70x + 0.03x^2 + 0.86x^3$	44.88
$\epsilon_{0\nu}$	13.18	$13.18 - 3.12x$	10.06
$\epsilon_{\infty\nu}$	10.89	$10.89 - 2.73x$	8.16

The confining potential for the electron is $U = 600 \times (1.155x + 0.37x^2)$ meV. We chose the effective atomic unit so that the unit of length is the effective Bohr radius $a_0^* = \epsilon\hbar^2/m^*e^2$ and the unit of energy is the effective Rydberg $R^* = m^*e^4/2\hbar^2\epsilon^2$, which are about 100 Å and 5.25 meV respectively for GaAs. We have calculated the bound-polaron binding energy for different Al concentrations: $x = 0.1$ and 0.3 and different wire radii R_1. The radius of material 2 ($Ga_{1-x}Al_xAs$) R_2 is chosen to be far larger than R_1 (in this work, $R_2 = 20a_0^*$). In figure 1, we have plotted the binding energy E_b of the donor impurity state with electron–phonon coupling (bound polaron) versus the wire radius R_1 (solid lines). For comparison, we have also plotted the bound-polaron binding energy for infinite-well confinement (free-standing quantum wire) [10]. When R_1 increases, the bound-polaron binding energy reduces and reaches the three-dimensional limit regardless of the height of the confining potential. However, when R_1 is small, the bound-polaron binding energies in a finite-confinement quantum well wire behave differently to that for the infinite well. In the case of infinite confinement, the bound-polaron binding energy increases monotonically as R_1 reduces. But for finite confinement, as R_1 reduces, the bound-polaron binding energy first increases, then reaches a peak at a certain wire radius R_m and reduces thereafter. The higher the confining potential, the higher the value of the peak and the smaller the peak position value R_m. Because in the well with lower confining potential, the confinement effect is weaker, the electron wave function 'escapes' out of the wire and spreads into a wider space, causing a lower binding energy. For the same reason, the lines become even when the confining potential decreases. The dashed lines in figure 1 show the donor impurity binding energies (without a phonon contribution) under different confining potentials as functions of the wire radius. It is clear that the electron–phonon interaction has a great influence on the electron properties in the quantum well wire systems. To investigate the phonon influence in detail, in figure 2 we have plotted the contributions of different phonon modes (LO1, LO2, IO) to the bound-polaron binding energy. In the figure we can see that most of the phonon contribution to the bound-polaron binding energy comes from the electron–IO phonon interaction. ΔE_{IO} is very small when the radius of the wire

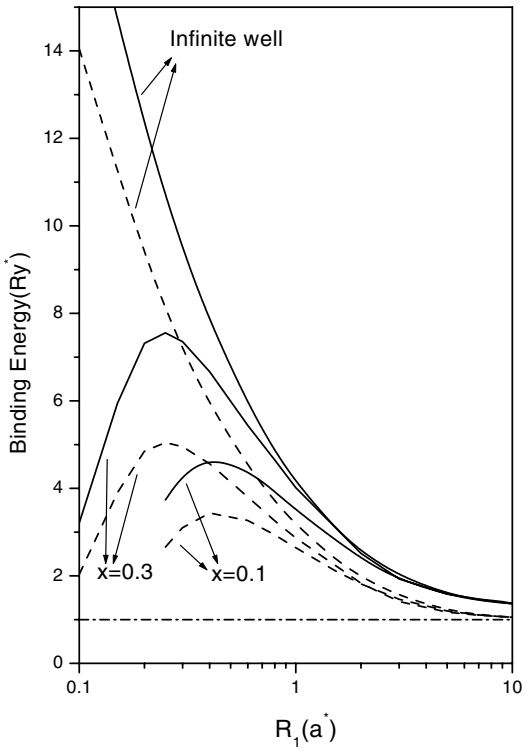

Figure 1. Binding energies of the donor impurity as functions of the wire radius. Dashed curves: the bare electron without the phonon contribution; solid curves: with the phonon contribution.

R_1 is large, then increases quickly as R_1 reduces. It reaches a peak and then decays quickly as the wire becomes narrower, because for the case of small R_1, the electron wave function spreads into the barrier area and hence reduces the effect of the electron–IO phonon interaction. Compared to that of the IO phonon modes, the contributions of the LO phonon modes are far less important. The contribution of the LO modes inside the wire (ΔE_{LO1}), which depends on the electron wave function inside the wire, increases as R_1 increases and becomes dominant at the three-dimensional limit. One could observe that the curve for ΔE_{LO1} is a little concave when R_1 is larger than 1. This could be explained by the coupling between the LO1 eigenmodes and the electron (the mathematical analysis is a little bit lengthy, so we put it in appendix B). In contrast, ΔE_{LO2}, which is related to the electron wave function in the barrier area, hardly makes any contribution to the bound-polaron binding energy until the well is quite narrow. However, it obviously increases as R_1 reduces. This shows that when studying the properties of the quantum well wire system, it is unnecessary to take the LO phonon modes in the barrier area into consideration when the well is not very narrow.

6. Summary

In conclusion, we have investigated the impurity binding energy in a cylindrical quantum well wire with a finite confining potential. In order to study the influence of electron–phonon interaction in the system, we worked out the expressions for various phonon modes and the electron–phonon interaction Hamiltonians in this quantum well wire system. We found out

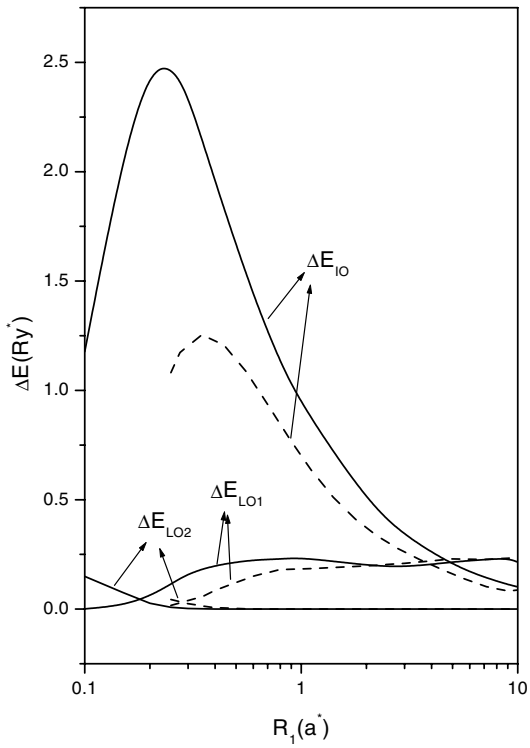

Figure 2. Contributions of different phonon modes to the bound-polaron binding energy. Different confining potential heights (Al concentration x) are used: solid curves: $x = 0.3$; dashed curves: $x = 0.1$.

that there exist two types of confined longitudinal phonon mode. One is in the well material (LO1), another in the barrier materials (LO2). We have also derived the dispersion relation for the interface optical phonon modes. We studied the contribution of electron–phonon coupling to the impurity binding energy in this quantum well wire system. It is found that the electron–phonon interaction contributes greatly to the impurity binding energy. For example, the total phonon contribution to the impurity binding energy (E_b) for a GaAs/$Ga_{0.7}Al_{0.3}As$ quantum well wire could be as much as 33% of E_b at $R_1 = 0.25$ (figure 1). Detailed analysis shows that the interface phonon modes play a major role in the phonon contributions, especially when the radius of the wire is relatively small. The contributions of the LO phonon modes are less important, especially that of the mode in the barrier material (LO2). In fact, the LO2 modes do not show an influence on the binding energy until the wire is quite narrow, while the influence of the LO1 modes increase as the radius of the wire increases. When the radius of the wire becomes very large, ΔE_{LO1} reaches a certain limit value, which is the three-dimensional limit [10].

Acknowledgments

This work was financially supported by the Natural Science Foundation of Guangdong Province, China.

Appendix A. The orthogonality of T_{ml}

We now prove that $T_{ml}(a_{ml}\rho/R_1)$ and $T_{mk}(a_{mk}\rho/R_1)$ are orthogonalized within the range of $R_1 \leqslant \rho \leqslant R_2$.

As $T_{ml}(a_{ml}\rho/R_1)$ is defined by equation (25), it satisfies the following Bessel equation:

$$\rho^2\frac{\mathrm{d}^2T_{ml}(a_{ml}\rho/R_1)}{\mathrm{d}\rho^2}+\rho\frac{\mathrm{d}T_{ml}(a_{ml}\rho/R_1)}{\mathrm{d}\rho}+\left(\frac{a_{ml}^2}{R_1^2}\rho^2-m^2\right)T_{ml}(a_{ml}\rho/R_1)=0 \tag{A1}$$

and $T_{mk}(a_{mk}\rho/R_1)$ satisfies

$$\rho^2\frac{\mathrm{d}^2T_{mk}(a_{mk}\rho/R_1)}{\mathrm{d}\rho^2}+\rho\frac{\mathrm{d}T_{mk}(a_{mk}\rho/R_1)}{\mathrm{d}\rho}+\left(\frac{a_{mk}^2}{R_1^2}\rho^2-m^2\right)T_{mk}(a_{mk}\rho/R_1)=0. \tag{A2}$$

Multiplying equation (A1) by $T_{mk}(a_{mk}\rho/R_1)/\rho$, and equation (A2) by $T_{ml}(a_{ml}\rho/R_1)/\rho$, we get

$$\begin{aligned}&\rho T_{mk}(a_{mk}\rho/R_1)\frac{\mathrm{d}^2T_{ml}(a_{ml}\rho/R_1)}{\mathrm{d}\rho^2}+T_{mk}(a_{mk}\rho/R_1)\frac{\mathrm{d}T_{ml}(a_{ml}\rho/R_1)}{\mathrm{d}\rho}\\&\qquad+\left(\frac{a_{ml}^2}{R_1^2}\rho-\frac{m^2}{\rho}\right)T_{mk}(a_{mk}\rho/R_1)T_{ml}(a_{ml}\rho/R_1)=0\end{aligned} \tag{A3}$$

$$\begin{aligned}&\rho T_{ml}(a_{ml}\rho/R_1)\frac{\mathrm{d}^2T_{mk}(a_{mk}\rho/R_1)}{\mathrm{d}\rho^2}+T_{ml}(a_{ml}\rho/R_1)\frac{\mathrm{d}T_{mk}(a_{mk}\rho/R_1)}{\mathrm{d}\rho}\\&\qquad+\left(\frac{a_{mk}^2}{R_1^2}\rho-\frac{m^2}{\rho}\right)T_{ml}(a_{ml}\rho/R_1)T_{mk}(a_{mk}\rho/R_1)=0\end{aligned} \tag{A4}$$

and subtracting (A3) from (A4) and integrating both sides of the equation from R_1 to R_2 yields

$$\begin{aligned}&\int_{R_1}^{R_2}\left[\left(\frac{a_{ml}^2}{R_1^2}-\frac{a_{mk}^2}{R_1^2}\right)\rho\right]T_{ml}(a_{ml}\rho/R_1)T_{mk}(a_{mk}\rho/R_1)\,\mathrm{d}\rho\\&\qquad=\left[\rho\left(T_{ml}(a_{ml}\rho/R_1)\frac{\mathrm{d}T_{mk}(a_{mk}\rho/R_1)}{\mathrm{d}\rho}-T_{mk}(a_{mk}\rho/R_1)\frac{\mathrm{d}T_{ml}(a_{ml}\rho/R_1)}{\mathrm{d}\rho}\right)\right]_{R_1}^{R_2}.\end{aligned} \tag{A5}$$

That is

$$\begin{aligned}&\left(\frac{a_{ml}^2}{R_1^2}-\frac{a_{mk}^2}{R_1^2}\right)\int_{R_1}^{R_2}T_{ml}(a_{ml}\rho/R_1)T_{mk}(a_{mk}\rho/R_1)\rho\,\mathrm{d}\rho\\&\qquad=\left[\rho\left(\frac{a_{ml}}{R_1}T_{m+1,l}(a_{ml}\rho/R_1)T_{mk}(a_{mk}\rho/R_1)\right.\right.\\&\qquad\quad\left.\left.-\frac{a_{mk}}{R_1}T_{ml}(a_{ml}\rho/R_1)T_{m+1,k}(a_{mk}\rho/R_1)\right)\right]_{R_1}^{R_2}\\&\qquad=\left[\rho\left(\frac{a_{ml}}{R_1}T_{ml}(a_{ml}\rho/R_1)T_{m-1,k}(a_{mk}\rho/R_1)\right.\right.\\&\qquad\quad\left.\left.-\frac{a_{mk}}{R_1}T_{m-1,l}(a_{ml}\rho/R_1)T_{mk}(a_{mk}\rho/R_1)\right)\right]_{R_1}^{R_2}\equiv 0.\end{aligned} \tag{A6}$$

We have made use of the recurrence relation

$$T_m'(x)=\frac{m}{x}T_m(x)-T_{m+1}(x)$$

and the boundary conditions at $\rho=R_1$ and $\rho=R_2$ (equation (26)).

So

$$\int_{R_1}^{R_2} T_{ml}(a_{ml}\rho/R_1)T_{mk}(a_{mk}\rho/R_1)\rho\,\mathrm{d}\rho \begin{cases} = 0 & \text{if } l \neq k \\ \neq 0 & \text{if } l = k \end{cases}$$

and

$$\int_{R_1}^{R_2} T_{m-1,l}(a_{ml}\rho/R_1)T_{m-1,k}(a_{mk}\rho/R_1)\rho\,\mathrm{d}\rho \begin{cases} = 0 & \text{if } l \neq k \\ \neq 0 & \text{if } l = k. \end{cases}$$

Appendix B. The LO1 eigenmodes and the electron wave function

From equation (71) we learn that only the $m = 0$ modes will couple with the electron wave function.. The LO1 phonon modes are characterized by l, which is the number of zeros within $0 < \rho < R_1$. In figure A1 we have plotted the functions of the first four eigenmodes. We notice that the amplitude of the eigenmode function decays quickly, and it becomes more and more oscillating as l increases. ΔE_{LO1} in equation (71) depends on the coupling between the electron wave function and the phonon eigenmodes. In figure A2 we have plotted the radial electron probability distribution function $w(\rho)$ for some R_1-values. $w(\rho)$ is defined by

$$w(\rho)\,\mathrm{d}\rho = 2\pi\left[\int_{-\infty}^{\infty} |\Phi(\rho, z)|^2\,\mathrm{d}z\right]\rho\,\mathrm{d}\rho.$$

As R_1 increases, the maximum position (ρ_M) of $w(\rho)$ will get closer to the centre of the quantum wire. When R_1 is very small, the distribution gives $\rho_M > R_1$; that is, the major part of the electron wave function lies outside the quantum wire, which is beyond the influence of the LO1 phonon modes. However, considering that we are using relative units in figure A2,

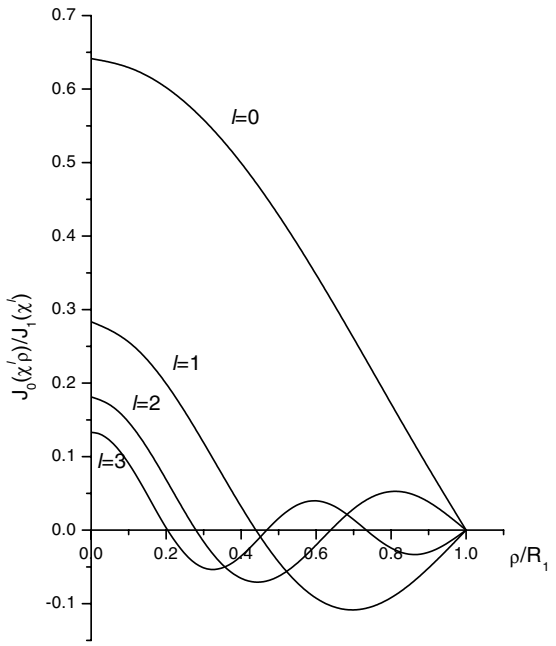

Figure A1. The LO1 eigenmodes.

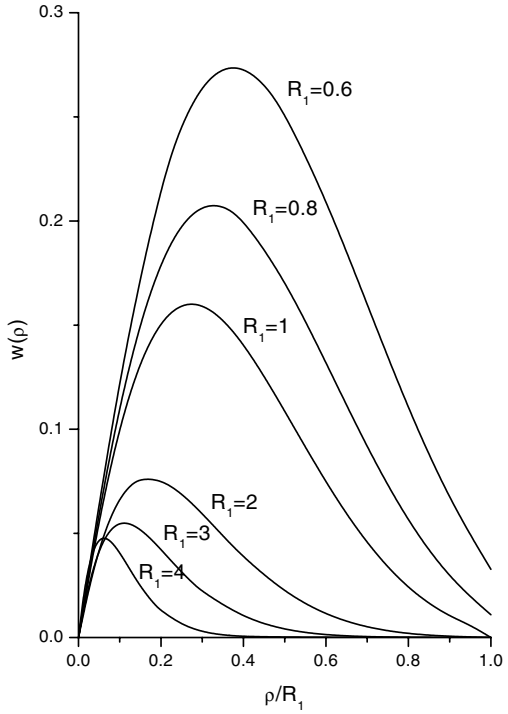

Figure A2. The radial distribution of the electron wave function.

the actual position of ρ_M changes little with R_1. This means that, as R_1 increases, the influence of the LO1 phonon modes becomes significant as the electron 'falls' into the quantum wire (figure 2). The total contribution of the LO1 phonon modes in equation (71) is a summation over all LO1 eigenmodes. Considering the oscillating nature of the higher-l modes, when R_1 is small, only the contribution of the very low modes affects ΔE_{LO1}. And the contribution of each single mode increases steadily as R_1 increases until $R_1 = 1$. After that, all of the electron wave function distributes within the quantum wire and ρ_M gets closer and closer to the centre of the quantum wire as R_1 increases. One can also see that when R_1 increases, the value of $w(\rho)$ reduces. Considering the properties of the eigenmode function in figure A1, it is easy to understand that the contribution of each single mode starts to decrease as R_1 increases. At the same time, because ρ_M gets closer to the centre of the wire and $w(\rho)$ decreases and finally vanishes as ρ increases, more and more eigenmodes start to make significant contributions to ΔE_{LO1}. The competition between these two factors results in a little concavity in the curve for ΔE_{LO1}.

References

[1] Yu SeGi, Pevzner V B, Kim K W and Stroscio M A 1998 *Phys. Rev.* B **58** 3580
[2] Kash K, Scherer A, Worlock J M, Craighead H G and Tamargo M C 1986 *Appl. Phys. Lett.* **49** 1043
[3] Kubena R L, Joyce R J, Ward J W, Garvin H L, Straton F P and Brault R G 1987 *Appl. Phys. Lett.* **50** 1959
[4] Villamil P and Montenegro N P 1998 *J. Phys.: Condens. Matter* **10** 10 599
[5] Montenegro N P, Gondar J L and Oliveira L E 1991 *Phys. Rev.* B **43** 1824
[6] Bastard G 1981 *Phys. Rev.* B **24** 4714
[7] Green R L and Bajaj K K 1982 *Solid State Commun.* **45** 825

[8] Maihiot C and Chang Y C 1982 *Phys. Rev.* B **26** 4449
[9] Brown J W and Spector H N 1986 *J. Appl. Phys.* **59** 1179
[10] Xie H J, Chen C Y and Ma B K 2000 *Phys. Rev.* B **61** 4827
[11] Hai G Q, Peeters F M and Devreese J T 1990 *Phys. Rev.* B **42** 11 063
[12] Pokatilov E P, Klimin S N, Balaban S N and Fomin V M 1995 *Phys. Status Solidi* b **191** 311
[13] Chen C Y, Jin P W, Li W S and Lin D L 1997 *Phys. Rev.* B **56** 14 913
[14] Chen C Y, Li W S and Jin P W 1997 *Commun. Theor. Phys.* **28** 9
[15] Xie H J and Chen C Y 1998 *Eur. Phys. J.* B **5** 215
[16] Lucas A A, Kartheuser E and Bardro R G 1970 *Phys. Rev.* B **41** 1439
[17] Licari J J and Evrard R 1977 *Phys. Rev.* B **15** 2254
[18] Wendler L 1985 *Phys. Status Solidi* b **129** 513
[19] Constantinou N C and Ridley B K 1990 *Phys. Rev.* B **41** 10 627
[20] Wang X F and Lei X L 1994 *Phys. Rev.* B **49** 4780
[21] Li W S and Chen C Y 1997 *Physica* B **229** 375
[22] Klimin S N, Pokatilov E P and Fomin V M 1995 *Phys. Status Solidi* b **190** 441
[23] Fomin V M and Pokatilov E P 1985 *Phys. Status Solidi* b **132** 69
[24] Wendler L and Grigoryan V G 1994 *Phys. Status Solidi* b **181** 133
[25] Wendler L and Grigoryan V G 1994 *Phys. Rev.* B **49** 14 531
[26] Pokatilov E P, Fomin V M, Balaban S N, Klimin S N and Devreese J T 1998 *Phys. Status Solidi* b **210** 879
[27] Wendler L and Hartwig B 1990 *J. Phys.: Condens. Matter* **2** 8847
[28] Bennett C R, Constantinou N C, Babiker M and Ridley B K 1995 *J. Phys.: Condens. Matter* **7** 9819
[29] Xie H J and Chen C Y 1994 *J. Phys.: Condens. Matter* **6** 1007
[30] Xie H J, Chen C Y and Liang S D 1995 *Phys. Rev.* B **52** 1776
[31] Chuu D S and Lou Y C 1990 *Phys. Rev.* B **43** 14 504